

Segmentation and Classification of Dermoscopic Skin Cancer on Green Channel

Hind Abouche

*MECATronique Team, CPS2E Laboratory
National Superior School of Mines
Rabat, Morocco*

hind.abouche@enim.ac.ma

Anwar Jimi

*MECATronique Team, CPS2E Laboratory
National Superior School of Mines
Rabat, Morocco*

anwar.jimi@enim.ac.ma

Nabila Zrira

*ADOS Team, LISTD Laboratory
National Superior School of Mines
Rabat, Morocco*

zrira@enim.ac.ma

Ibtissam Benmiloud

*MECATronique Team, CPS2E Laboratory
National Superior School of Mines
Rabat, Morocco*

benmiloud@enim.ac.ma

Abstract—Melanoma the most dangerous type of skin cancer, has been on the rise in recent years. Hands-on identification of melanoma in its early stages with the unaided eye is error-prone and necessitates extensive expertise and experience. Due to the scarcity of skilled dermatologists, a computerized and automated technique is required to effectively identify melanoma. The following approach attempts to accomplish this task by creating a new approach capable of segmenting, then classifying melanoma. The procedure begins with the preparation of dermoscopic images to remove hairs using the Dull Razor algorithm, followed by image segmentation, in which we computed the Hausdorff Distance, Dice, and Jaccard coefficients to determine which channel of the RGB space was best to utilize to separate the skin lesion from the background. The segmented images using the green channel are then utilized to calculate the Gray Level Co-occurrence Matrices (GLCM) and to extract the color characteristics of the region of interest. Our approach is able to achieve a Dice coefficient and an accuracy of 95% on the PH2 dermoscopic images.

Index Terms—Melanoma, Green channel, GLCM, Color features, PH2

I. INTRODUCTION

Skin cancer is one of the most common and life-threatening cancers all over the world, especially since its frequency is increasing with the decrease in ozone levels. In most cases, skin cancer is related to exposure to unprotected sunlight that sends ultraviolet radiation [1]. The more the ozone layer loses the protective filtering function, the more harmful solar ultraviolet rays reach the earth's surface. According to statistics, for every 10% reduction in ozone levels, 300,000 non-melanoma cases, and over 4,000 melanoma cases are recorded [2].

There are two main types of skin cancer: melanoma (i.e., the malignant one) and non-melanoma (i.e., the benign one). According to the worldwide health organization [3] there are two to three million non-melanoma cases and more than 130,000 melanoma cases that occur globally yearly. Skin cancer is called benign when the mole on the skin shows any

IEEE/ACM ASONAM 2022, November 10-13, 2022
978-1-6654-5661-6/22/\$31.00 © 2022 IEEE

non-cancerous growth, as opposed to malignant melanoma, which shows cancerous growth of the mole on the skin.

The most severe and deadly form of skin cancer is malignant melanoma. It is the worst type of skin cancer and develops from a malignant development in a skin lesion that is pigmented and causes 75% of all skin cancer deaths [4]. According to World Cancer Research Fund International [2], the 17th most prevalent cancer worldwide is cutaneous melanoma. There were more than 150,000 new instances of melanoma of the skin in 2020. It is the 15th most prevalent cancer in women and the 13th most common cancer in males.

Diagnosis of malignant melanoma at an earlier stage is critical for dermatologists. Unfortunately, it might be challenging to assess aspects visually before identifying a malignant pigmented tumor. Even seasoned dermatologists struggle to tell the difference between melanoma and other pigmented skin lesions, like benign moles and the more common ones [5].

Skin cancer may be found in two ways: by utilizing computers or by consulting professionals. Visual inspection of dermoscopic images is used to search for skin lesions and wounds. They examine the scars, among other things, to see whether they are not healing and if their growth is uneven with hazy borders [6]. By analyzing photographs taken with common digital cameras or images from dermatoscopy tests, skin cancer may also be automatically detected.

The cost of manually diagnosing skin cancer is high. According to the Skin Cancer Foundation [5], treating skin cancer in the United States costs an estimated \$8.1 billion annually, of which \$4.8 billion is spent on treating non-melanoma skin cancer and \$3.3 billion is spent on treating melanoma.

Computers are not smarter than humans, but they may be able to extract information, such as textural features, that are not always simple for the human eye to detect. As a result, dermoscopy is now being enhanced with computer vision and image processing techniques in order to produce equipment that is sufficiently effective for the correct diagnosis of lesions,

seeking help with the goal of obtaining exact data to assist the experts [7]. With this improvement, it is possible to easily classify different lesion types and identify lesions, borders, and colors.

The accuracy of clinical diagnosis can be improved by this technology by providing new morphological criteria for the identification of skin lesions. Dermoscopy image diagnoses, however, may be arbitrary or erroneous, even by experienced dermatologists [8]. It is essential to investigate automated techniques for precise skin lesion segmentation.

In our work, we conducted a thorough investigation of the performance of the green channel for skin cancer segmentation and feature extraction for lesion diagnosis. The main contributions are stated below:

- Image segmentation using the green channel mask instead of the whole RGB space;
- GLCM parameters such as contrast, energy, homogeneity, entropy, and correlation are recovered from the PH2 dataset;
- Color characteristics are taken from each color plane (red, green, and blue) and used as statistical features. These are the mean, variance, skewness, and standard deviation;
- As a result, GLCM and color features are employed as consolidated features to assess performance using different GLCM offsets (2, 4, 8, 12, 16, 20, 24, 28).

The following is the structure of the research paper. Section 2 summarizes previous work in the field of skin cancer classification. Section 3 covers all stages of skin cancer detection, from image preprocessing to image classification. Section 4 discusses the research work's implementation specifics and the experimental findings. Section 5 closes the paper with a conclusion and possible future work.

II. RELATED WORK

Recently, several approaches have been proposed to evaluate the use of dermoscopic images for skin lesion classification issues, in this section we provide a brief description of the related works that highlight skin cancer classification. Sheha et al. [9] used the GLCM features as well as Multilayer perceptron classifier (MLP) to detect whether the lesion is Melanocytic Nevi or Malignant melanoma. In the training, the MLP achieved an accuracy of 100 %, while in the testing the traditional MLP reached 92 %. Sumithra et al. [10] used three main features including texture, color, and RGB Histogram. The performance of the system was tested on their own dataset of 726 samples divided into five different classes of diseases. The results showed 46.71% and 34% of F-measure using SVM and k-NN classifier, respectively. F-measure achieved 61% when fusing SVM and k-NN. Using the DermIs dataset and SVM as a classifier, Almansour and Jaffar [11] presented a comparison of performance (i.e., accuracy) between a different set of features to detect the skin lesion including, GLCM (85%), Local binary Patterns(LBP) (83%), Color (87%), the combination of LPB and GLCM (87%). Also, they combined LBP, GLCM, and Color features that achieved an accuracy of 90.32%. Almaraz-Damian et al. [12] used the texture,

color, and ABCD (Asymmetry, Border, Color, Diameter) rule to extract the shape features. They also used the k-means algorithm for the classification procedure. The method was applied to DermQuest and Dermatology Information System providing a performance of 75.1%. Ashfaq et al. [13] utilized the ABCD rule and the statistical parameters of GLCM with a different set of offsets as characteristics of the images. Both dermIS and dermQuest were used as a dataset for this work. The classification between Melanoma and Non-Melanoma was divided into two experiments: the first one was based on using GLCM features and color features which reached an accuracy of 80%, in the second one only the ABCD features were used achieving an accuracy of 93%. Moura et al. [14] proposed a model based on the ABCD (Asymmetry, Border, Color, and Diameter) rule for feature extraction, and a pre-trained Convolutional Neural Network. As a result, the model reached an accuracy of 94.9%. In the approach proposed by Majumder and Ullah [15], the prediction of skin lesions type was done based on 8 features of the ABCD rule on the PH2 dataset. The results were analyzed according to accuracy (98%), specificity(98%), and sensitivity (97.5%). In another study, Zaqout [16] used TDS (total dermoscopic score) and the ABCD features on the PH2 dataset. Results showed that this system achieved a sensitivity rate of 85%, specificity of 92%, and accuracy of 90%. More recently, Senan et al. [17] used a preprocessing technique to remove noise, hair, and air bubbles. After the segmentation phase, a morphological method was used to enhance the segmented images to extract the ABCD features. They tested the proposed method on the PH2 dataset. They obtained an accuracy of 84% for two classes Malignant and Benign. In the approach proposed Tumpa et al. [18], the prediction of skin lesions type as benign or malignant was performed from a system based on ABCD features combined with GLCM and LBP features. The input images are obtained from the ISIC archive dataset and PH2 dataset.

III. METHODOLOGY

The suggested pipeline for differentiating between malignant and benign skin cancer is shown in Fig. 1. PH2 dataset is used to gather the input dermoscopic dataset. The approach consists of the following key steps: image preprocessing, green channel conversion, Region of Interest (RoI) segmentation, feature extraction, and classification.

A. Dermoscopic images

The collection of appropriate input datasets is critical for the effective implementation of the next phases and the eventual development of a consistent and robust automated diagnostic system for melanoma lesions. The input dataset must contain all forms of possible lesion images. Dermoscopy images were acquired from the PH2 dataset, which was created by a combined research partnership of the University of Porto and the Dermatology Service of Pedro Hispano Hospital in Portugal [19]. The dataset is publicly available on the internet for any research to utilize as a standard. We gathered 200 melanocytic images from this dataset, which we split into

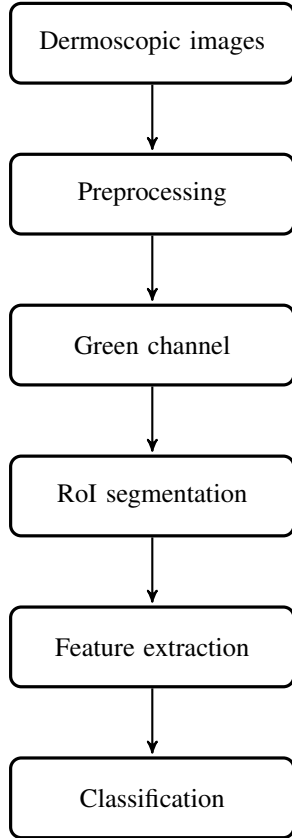


Fig. 1. The flowchart of our proposed approach

two groups: 160 benign lesions (including 80 common and 80 atypical nevus) and 40 malignant lesions. These images were captured under the same settings using the Tuebinger mole analyzer equipment and have the same characteristics??:

- 8-bit RGB pictures
- Bitmap format: BMP
- Resolution: 764×574 pixels

Figure III-A shows the two types of lesions from dataset PH2, a and b are benign nevus, c and d are malignant melanoma

B. Preprocessing

Excessive hair and the diversity of its color, shape, and direction on lesions in dermoscopy images can make it difficult to spot injuries, thus getting rid of it is a crucial element of the preprocessing stage. As shown in Figure III-B, hairs in dermoscopy images are eliminated using an algorithm called Dull Razor that was developed by Lee et al. [20]. Listed below are the steps in this algorithm:

- Step 1: Make the original image grayscale;
- Step 2: Apply the Black Hat filter on the grayscale image to locate the hair contours;
- Step 3: Repaint the original image using the mask.

C. Green channel

We focus on the image segmentation stage in this work because most earlier approaches used the whole RGB space

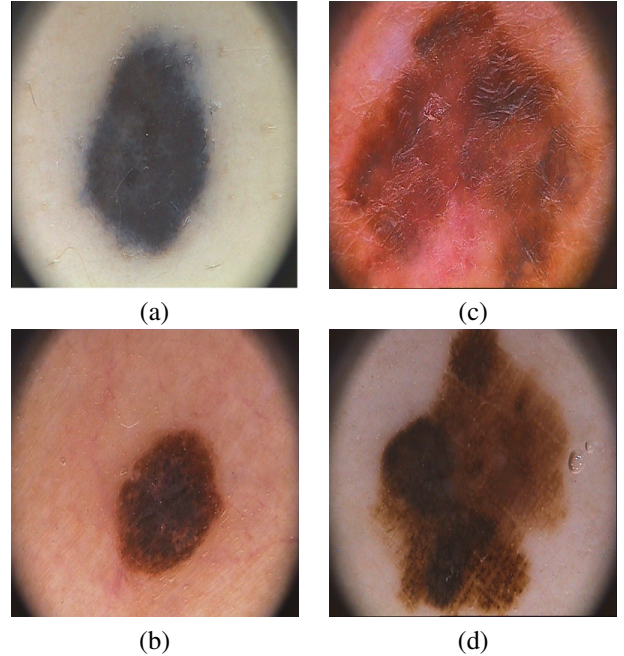


Fig. 2. Left : (a) and (b) are benign tumor, Right: (c) and (d) are malignant tumor

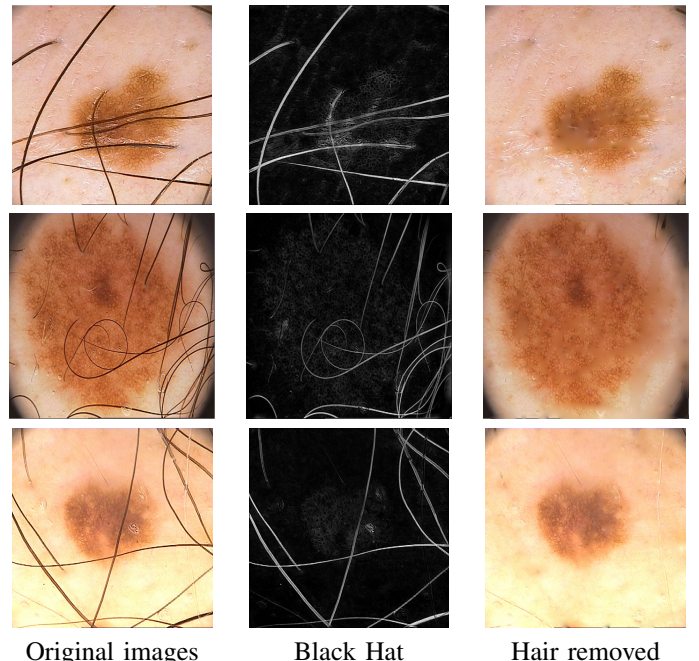


Fig. 3. Left: image with hair. Right: image after hair removal

to separate the lesion from the background. We came up with the notion of dividing the RGB image into three channels and seeing what we could achieve visually.

Figure III-C clearly shows that some color information was lost in the grayscale, red, and blue channels, but the green channel is the one that keeps the color variation across the whole surface of the image.

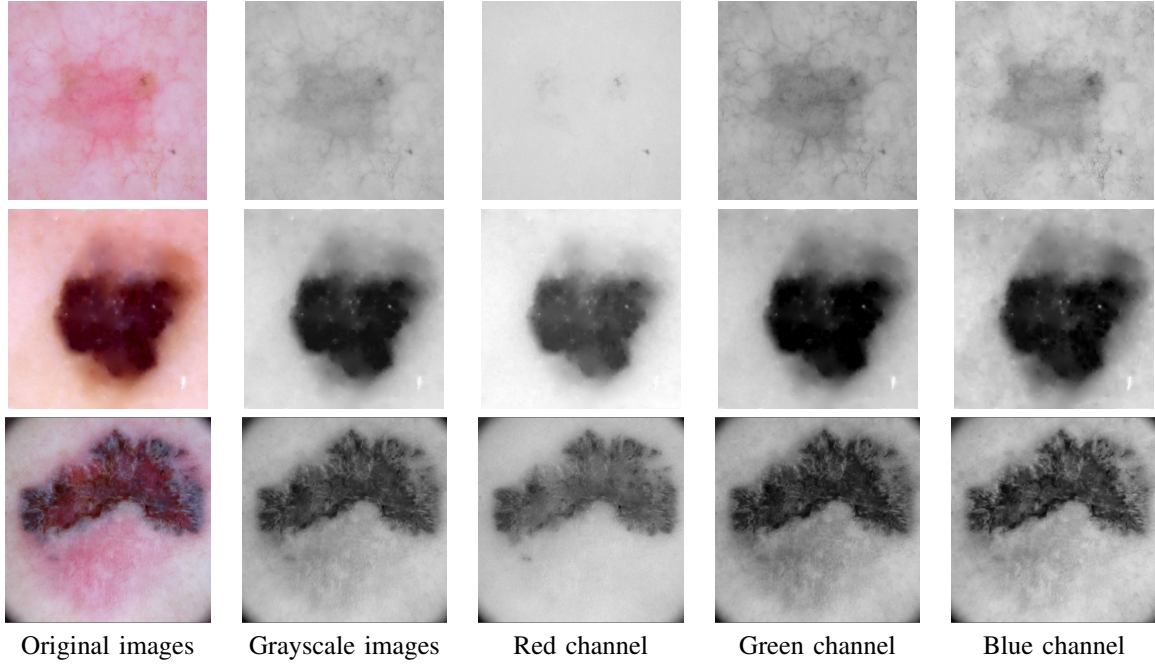


Fig. 4. Comparaison of each RGB channel and grayscale

D. ROI segmentation

Segmentation classifies the pixels of the image into distinctive categories. In cases of skin cancer detection, segmentation extracts the lesion boundary that divides it from the surrounding non-cancerous tissue. A binary mask at the site of the lesion is the segmentation's output. In this work, we used Dice, Jaccard, and Hausdorff distance to select the best channel so we could use its mask to segment the lesion from the background.

E. Feature extraction

The next step is to extract important and distinctive characteristics from the segmented lesion once the ROI has been separated.

We depict lesion regions in this work using information from texture and color space. Because color and texture are the sole traits that predominate in the lesion region, these characteristics were chosen.

By mapping the gray level co-occurrence probabilities based on the spatial relationships of pixels in various angular orientations, we were able to extract: contrast, correlation, energy, entropy, and homogeneity. Whereas, for the color features, we compute the Mean, Skewness, Standard Deviation, and Variance for each channel in the RGB color space.

1) *Texture Features*: The texture of skin is a natural characteristic that contains information on the structure or pattern arrangement of skin. The link between the gray values of the picture space and the spatial neighborhood pixels is shown by texture features.

Entropy, Energy, Contrast, Correlation, and Homogeneity, which are obtained from a GLCM matrix, are five of the traditional statistical texture measurements used by Haralick et

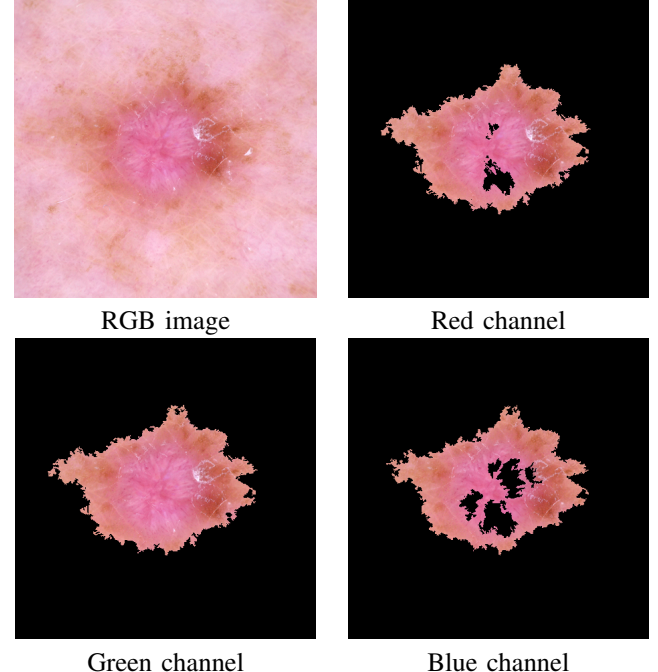


Fig. 5. Lesion segmentation on each channel

al. [21]. The GLCM is a table that shows how frequently various pixel luminance value combinations (sometimes known as "gray levels") appear in a particular pixel pair of a picture. In order to determine the locative dependency of brightness (gray-level) values, which aids in discovering important details about the nearby pixels in an image, a two-dimensional gray-level co-occurrence matrix is often and extensively utilized in

the area of texture analysis.

Four orientations are taken into account for each pixel in this work, including 0°, 45°, 90°, and 135° with offsets of 2, 4, 8, 12, 16, 20, 24, and 28. The average values are then employed as the final Haralick features and are calculated as follows :

Contrast measures the spatial frequency of an image. It is the distinction in the GLCM instant. The difference between the highest and lowest values of a continuous collection of pixels is referred to as contrast. It counts the number of local differences in an image.

$$Contrast = \sum_i \sum_j (i - j)^2 P(i, j) \quad (1)$$

Energy is the sum of squared components in the GLCM matrix. It is also known as the uniformity or the angular second moment.

$$Energy = \sum_i \sum_j P(i, j)^2 \quad (2)$$

Homogeneity is a measure of how near the distribution of items in GLCM is to its diagonal. It's also known as the Inverse Difference Moment. When all of the components are the same, homogeneity is maximized.

$$Homogeneity = \sum_i \sum_j \frac{P(i, j)}{1 + (i - j)^2} \quad (3)$$

Correlation is a measure of how linked a pixel is to its neighbors throughout the entire image.

$$Correlation = \frac{[\sum_i \sum_j (ij)P(i, j)] - \mu_x \mu_y}{\sigma_x \sigma_y} \quad (4)$$

Entropy which is calculated as follows:

$$Entropy = \sum_i \sum_j P(i, j) \ln(P(i, j)) \quad (5)$$

Equations 1–5 depict four GLCM properties, namely Contrast, Energy, Homogeneity, Correlation, and Entropy, where $P(i, j)$ is the normalized entry in row i and column j of the GLCM, and I is the intensity of one pixel while j is that of the next pixel constituting the pair for GLCM.

2) *Color Features*: One important characteristic for diagnosing skin diseases is color. Basically, a difference in skin tone is the first indicator that may be used to distinguish between benign and malignant melanoma in dermoscopic images.

"Color" is the appearance of an item when exposed to light. Studying the three main colors, such as red, green, and blue, helped us understand the concept of color space. Using the color feature approach, the segmented lesion areas' exhibited colors are to be identified. This was done by taking the Mean, Standard Deviation, Variance, and Skewness from the segmented lesion regions.

The four properties mentioned above are computed across each individual channel, yielding 12 color features when the

following two factors are combined: The four features (from every channel) were multiplied by 3 channels in RGB color space, and they were retrieved as follows :

Mean is the average value, which is calculated by adding all of the observed outcomes from the sample and dividing by the total number of events.

$$M = \frac{1}{x} \sum_{i=1}^x P \quad (6)$$

Standard Deviation: is the distance between data values and the mean.

$$STD = \sqrt{\frac{1}{x} \sum_{i=1}^x (P_j - M)^2} \quad (7)$$

Skewness: is the degree of asymmetry in the distribution which is computed by:

$$Skewness = \sqrt[3]{\frac{1}{x} \sum_{i=1}^x (P_j - M)^3} \quad (8)$$

Variance: refers to the variety in color distribution.

$$S = \frac{1}{x} \sum_{i=1}^x (P_j - M)^2 \quad (9)$$

Where P_j represents the j^{th} pixel of a color channel P in a color space of an image I with x pixels.

F. Classification

Following feature extraction, the next step is to train a model utilizing the retrieved features from the 200 dermoscopic images from the PH2 dataset. The skin lesion identification function in this work may be thought of as a normal binary categorization problem since there are two types of melanoma lesions (i.e., malignant or benign melanoma). The goal is to assign a suitable class label to each skin lesion in the provided dermoscopic images.

In this work, we chose the supervised learning algorithm Support Vector Machine (SVM) [22] as a classifier since it interprets pictures quickly and effectively. Support Vector Machine, or SVM, is a common supervised learning technique for classification and regression issues [23]. However, it is mostly utilized for classification issues in Machine Learning. The SVM classifier is also capable of recognizing and classifying complex data patterns.

The total number of inputs in this scenario is 17, of which 5 are extracted from GLCM and 12 are Mean, Variation, Skewness, and Standard Deviation for each of the red, green, and blue channels of the RoI. The target's label is either 1 or 0, with 0 indicating malignancy and 1 indicating benignity.

IV. EXPERIMENTAL RESULTS

In this section, we deploy qualitative as well as quantitative results of both skin lesion segmentation and feature classification.

A. Segmentation results

We employed three coefficients to confirm our assumption that the green channel provides the best near-mask to the ground truth for segmentation. They are as follows:

Hausdorff distance often known as the Hausdorff metric, is regularly used in image analysis to measure the distance between two subsets of a metric space. And it is computed by:

$$d_h(X, Y) = \max(d_{XY}, d_{YX}) \quad (10)$$

where

$$d_{XY} = \max_{x \in X} \min_{y \in Y} d(x, y) \quad (11)$$

$$d_{YX} = \max_{y \in Y} \min_{x \in X} d(x, y) \quad (12)$$

Dice Coefficient (DC) is both a geographical overlap indicator and a tool for validating repeatability. A DC value ranges from 0 to 1, with 0 indicating no spatial overlap and 1 representing total overlap. And it is calculated by:

$$DC = 2 \frac{|X \cap Y|}{|X| + |Y|} \quad (13)$$

Jaccard Coefficient The intersection of binary images X and Y divided by the union of X and Y is known as the Jaccard index. The Jaccard coefficient can have a value between 0 and 1, with 0 indicating no overlap and 1 representing the total overlap between the sets. And it is determined by:

$$JC = \frac{|X \cap Y|}{|X \cup Y|} \quad (14)$$

where X and Y are two different areas that we intend to measure their similarities.

Table I contains the results of the Dice and Jaccard coefficients, as well as the Hausdorff distance, which supports the segmentation results shown in Figure 6.

TABLE I
SEGMENTATION RESULTS WITH RESPECT TO THE CHANNEL

Channels	Dice	Jaccard	Hausdorff distance
RGB	0.91	0.87	6.32
Red	0.80	0.75	7.55
Green	0.95	0.90	6.12
Blue	0.90	0.85	7.30

B. Classification results

160 benign and 40 malignant lesion images were used for image-based classification analysis. The data split for training: test data is 80:20. The suggested approach accurately categorized all benign and malignant lesion images virtually. However, it missed a few. The model's efficacy is measured using four criteria: confusion matrix, accuracy, recall, f1-score, precision, and ROC (Receiver Operating Characteristic) curve.

Confusion matrix is a summary of classification problem prediction outcomes. The number of right and wrong predictions is summarized with count values and divided by class.

Accuracy of the model indicates how many times it was accurate overall:

$$\text{Accuracy} = \frac{TP + TN}{TP + FP + TN + FN} \quad (15)$$

Recall indicates how many times the model detected a certain category:

$$\text{Recall} = \frac{TP}{TP + FN} \quad (16)$$

Precision measures how well a model predicts a certain category:

$$\text{Precision} = \frac{TP}{TP + FP} \quad (17)$$

F1-score is a critical assessment statistic in machine learning. It succinctly summarizes a model's prediction effectiveness by combining two apparently opposing criteria: Precision and Recall.

$$F1 - Score = 2 \times \frac{\text{Precision} \times \text{Recall}}{\text{Precision} + \text{Recall}} \quad (18)$$

ROC curve (receiver operating characteristic curve) illustrates the performance of a classification model at all classification thresholds. It depends on two parameters: True Positive Rate (TPR) that represents also the recall, and False Positive Rate (FPR).

$$TPR = \frac{TP}{TP + FN} \quad (19)$$

$$FPR = \frac{FP}{FP + TN} \quad (20)$$

Where:

- **TP (True Positive)**: It is an abbreviation for malignant lesions that have been accurately diagnosed as malignant;
- **TN (True Negative)**: It assesses if benign lesions have been appropriately diagnosed as benign;
- **FN (False Negative)**: It stands for malignant tumors that were mistakenly recognized as benign;
- **FP (False Positive)**: It stands for benign lesions that were mistakenly diagnosed as malignant.

The SVM algorithm's purpose is to find the optimal line or decision boundary that can divide n-dimensional space into classes so that we may simply place fresh data points in the proper category in the future. This optimal choice boundary is referred to as a hyperplane [24].

Using the Grid Search approach, we were able to determine the ideal parameters of our model ($C= 10$, $\gamma=0.1$, kernel='linear'). By applying the SVM model, results for GLCM parameters with different offsets in the range of 2–28 were created, and the offset that produced the best results was chosen. Color characteristics were also employed to evaluate the SVM's performance. As depicted in Table II and ROC curve in Figure 7, the offset 4 gave the best results. As a consequence, the system achieves an overall classification accuracy of 95% and the Area under the ROC Curve (AUC) of 93%.

Our model produced extremely accurate predictions. According to the classification report depicted in Table III,

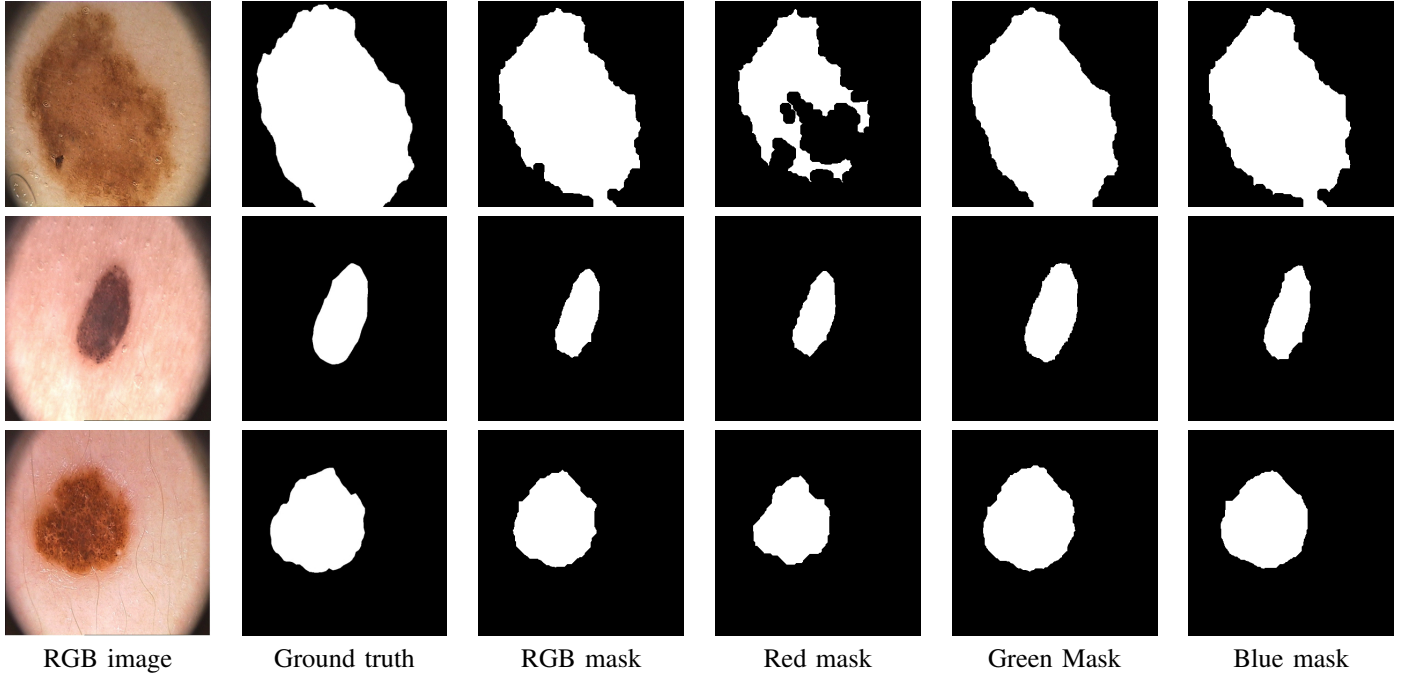


Fig. 6. Comparison of each channel mask and RGB mask to the ground truth

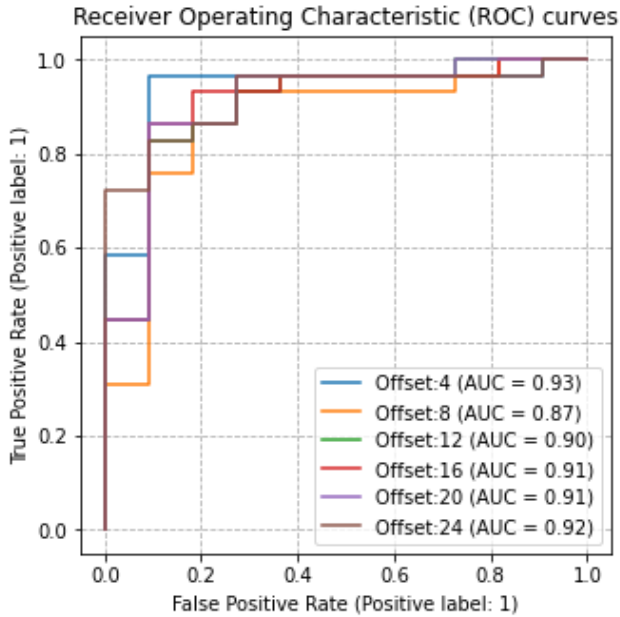


Fig. 7. ROC curve of different offset values

97% of the skin cancer cases predicted by the model to be benign were truly benign. And, of all the skin cancer cases predicted by the algorithm to be malignant, 91% were.

Our model performed admirably, as evidenced by the confusion matrix shown in Figure 8, which shows that it only predicted one tumor to be malignant but it turned out to be benign, and another to be benign but turned out to be

TABLE II
CLASSIFICATION RESULTS WITH RESPECT TO THE OFFSET VALUE

Offset	Accuracy	Precision	Recall
2	90%	90%	84%
4	95%	95 %	93.7%
8	82%	82%	73%
12	87.5 %	87.5 %	82.9 %
16	85%	85%	78.3%
20	87.5 %	87.5 %	82.9 %
24	90 %	90 %	84.6 %
28	87.5 %	87.5 %	82.9 %

TABLE III
THE CLASSIFICATION REPORT OF OUR PROPOSED APPROACH

Classes	Classification report			
	Precision	Recall	F1-score	Support
Malignant	91%	91 %	91 %	11
Benign	97%	97%	97 %	29
Average	95%	95 %	95%	40

malignant.

In Table IV, we compared the suggested approach's outcomes to those of other techniques on the PH2 dataset. To reduce noise, hair, and air bubbles, Senan et al. [17] employed preprocessing methods. Following the segmentation step, a morphological approach was utilized to improve the segmented pictures in order to obtain the ABCD characteristics. Their system reaches an accuracy of 84%. On the other hand, using the PH2 dataset, Zaqout [16] employed TDS and the ABCD characteristics. The results revealed that this method had a 90% accuracy rate, whereas our technique achieved an accuracy of 95%.

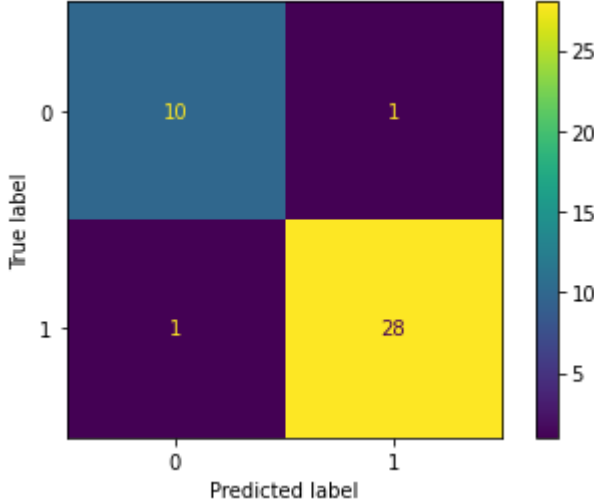


Fig. 8. Confusion matrix of our proposed approach

TABLE IV
COMPARISON WITH THE STATE-OF-THE-ART ON PH2 DATASET

Approach	Methodology	Accuracy
Zaqout [16]	Contrast Enhancing Segmentation thresholding ABCD features	90%
Senan et al. [17]	Gaussian filter Segmentation Morphological ABCD features TDS method	84%
Our approach	Dull Razor Green channel segmentation GLCM and Color features SVM	95%

V. CONCLUSION AND FUTURE WORK

In this work, an efficient skin lesion diagnosis strategy was proposed based on image segmentation on the green channel as well as hybrid texture and color features. Combining the characteristics enhances the accuracy of the categorization results. The Dull Razor algorithm is used to locate and eliminate the hair pixels in the image. The green channel of each image is used for segmentation, and various characteristics of the lesion are acquired using the GLCM and color feature extraction methods. The SVM identified the lesion as benign or malignant based on the target values of the input characteristics. This method should improve the efficacy of early diagnosis of melanoma malignancy. The suggested approach was tested on dermoscopic images from the PH2 dataset. The model achieved 95% overall accuracy.

However, a vast quantity of data will be examined in the future to improve training and classification accuracy, and a convolutional neural network will be used for melanoma classification. In addition, we want to apply the ABCD rule and LBP features to extract more features.

REFERENCES

- [1] R. Javed, M. S. M. Rahim, T. Saba, and A. Rehman, "A comparative study of features selection for skin lesion detection from dermoscopic images," *Network Modeling Analysis in Health Informatics and Bioinformatics*, vol. 9, no. 1, pp. 1–13, 2020.
- [2] (2022) Skin cancer statistics. [Online]. Available: <https://www.wcrf.org>
- [3] (2017) Radiation: Ultraviolet (uv) radiation and skin cancer. [Online]. Available: <https://www.who.int/fr>
- [4] E. Zagrouba and W. Barhoumi, "A preliminary approach for the automated recognition of malignant melanoma," *Image Analysis & Stereology*, vol. 23, no. 2, pp. 121–135, 2004.
- [5] (2022) Skin cancer information. [Online]. Available: <https://www.skincancer.org>
- [6] K. Lacy and W. Alwan, "Skin cancer," *Medicine*, vol. 41, no. 7, pp. 402–405, 2013.
- [7] N. Codella, J. Cai, M. Abedini, R. Garnavi, A. Halpern, and J. R. Smith, "Deep learning, sparse coding, and svm for melanoma recognition in dermoscopy images," in *International workshop on machine learning in medical imaging*. Springer, 2015, pp. 118–126.
- [8] M. Sadeghi, "Towards prevention and early diagnosis of skin cancer: computer-aided analysis of dermoscopy images," Ph.D. dissertation, Applied Science: School of Computing Science, 2012.
- [9] M. A. Sheha, M. S. Mabrouk, A. Sharawy *et al.*, "Automatic detection of melanoma skin cancer using texture analysis," *International Journal of Computer Applications*, vol. 42, no. 20, pp. 22–26, 2012.
- [10] R. Sumithra, M. Suhil, and D. Guru, "Segmentation and classification of skin lesions for disease diagnosis," *Procedia Computer Science*, vol. 45, pp. 76–85, 2015.
- [11] E. Almansour and M. A. Jaffar, "Classification of dermoscopic skin cancer images using color and hybrid texture features," *IJCSNS Int J Comput Sci Netw Secur*, vol. 16, no. 4, pp. 135–139, 2016.
- [12] J. Almaraz-Damian, V. Ponomaryov, and E. Rendon-Gonzalez, "Melanoma cade based on abcd rule and haralick texture features," in *2016 9th International Kharkiv Symposium on Physics and Engineering of Microwaves, Millimeter and Submillimeter Waves (MSMW)*. IEEE, 2016, pp. 1–4.
- [13] M. Ashfaq, N. Minallah, Z. Ullah, A. M. Ahmad, A. Saeed, and A. Hafeez, "Performance analysis of low-level and high-level intuitive features for melanoma detection," *Electronics*, vol. 8, no. 6, p. 672, 2019.
- [14] N. Moura, R. Veras, K. Aires, V. Machado, R. Silva, F. Araújo, and M. Claro, "Abcd rule and pre-trained cnns for melanoma diagnosis," *Multimedia Tools and Applications*, vol. 78, no. 6, pp. 6869–6888, 2019.
- [15] S. Majumder and M. A. Ullah, "Feature extraction from dermoscopy images for melanoma diagnosis," *SN Applied Sciences*, vol. 1, no. 7, pp. 1–11, 2019.
- [16] I. Zaqout, "Diagnosis of skin lesions based on dermoscopic images using image processing techniques," *Pattern Recognition-Selected Methods and Applications*, 2019.
- [17] E. M. Senan and M. E. Jadhav, "Analysis of dermoscopy images by using abcd rule for early detection of skin cancer," *Global Transitions Proceedings*, vol. 2, no. 1, pp. 1–7, 2021.
- [18] P. P. Tumpa and M. A. Kabir, "An artificial neural network based detection and classification of melanoma skin cancer using hybrid texture features," *Sensors International*, vol. 2, p. 100128, 2021.
- [19] T. Mendonça, M. Celebi, T. Mendonça, and J. Marques, "Ph2: A public database for the analysis of dermoscopic images," *Dermoscopy image analysis*, 2015.
- [20] T. Lee, V. Ng, R. Gallagher, A. Coldman, and D. McLean, "Dullrazor®: A software approach to hair removal from images," *Computers in biology and medicine*, vol. 27, no. 6, pp. 533–543, 1997.
- [21] R. M. Haralick, K. Shanmugam, and I. H. Dinstein, "Textural features for image classification," *IEEE Transactions on systems, man, and cybernetics*, no. 6, pp. 610–621, 1973.
- [22] M. A. Hearst, S. T. Dumais, E. Osuna, J. Platt, and B. Scholkopf, "Support vector machines," *IEEE Intelligent Systems and their applications*, vol. 13, no. 4, pp. 18–28, 1998.
- [23] C. Cortes and V. Vapnik, "Support-vector networks," *Machine learning*, vol. 20, no. 3, pp. 273–297, 1995.
- [24] M. d'Amico, M. Ferri, and I. Stanganelli, "Qualitative asymmetry measure for melanoma detection," in *2004 2nd IEEE International Symposium on Biomedical Imaging: Nano to Macro (IEEE Cat No. 04EX821)*. IEEE, 2004, pp. 1155–1158.